International Journal of Fluid Mechanics & Thermal Sciences
2022; 8(1): 10-22
http://www.sciencepublishinggroup.com/j/ijfmts
doi: 10.11648/j.ijfmts.20220801.12
ISSN: 2469-8105 (Print); ISSN: 2469-8113 (Online)

The Effect of Heat and Mass Transfer on Unsteady MHD Nanofluid Flow Through Convergent-Divergent Channel

Felicien Habiyaremye[1, *], Mary Wainaina[1], Mark Kimathi[2]

[1]Department of Mathematics and Actuarial Science, Catholic University of Eastern Africa, Nairobi, Kenya
[2]Department of Mathematics, Statistics and Actuarial Science, Machakos University, Machakos, Kenya

Email address:

fhabiyaremye@cuea.edu (F. Habiyaremye), nyawiragitoi@cuea.edu (F. Habiyaremye), memkimathi@gmail.com (M. Kimathi)
[*]Corresponding author

To cite this article:

Felicien Habiyaremye, Mary Wainaina, Mark Kimathi. The Effect of Heat and Mass Transfer on Unsteady MHD Nanofluid Flow Through Convergent-Divergent Channel. *International Journal of Fluid Mechanics & Thermal Sciences*. Vol. 8, No. 1, 2022, pp. 10-22.
doi: 10.11648/j.ijfmts.20220801.12

Received: April 7, 2022; **Accepted**: April 27, 2022; **Published**: May 10, 2022

Abstract: This paper investigates the effects of heat and mass transfer on unsteady MHD Nanofluid flow (silver-water) through convergent-divergent channel. The governing equations of this study are non-linear partial differential equations and these partial differential equations were reduced to ordinary differential equations. The resulting non-linear ordinary differential equations have been reduced to a system of first order of ordinary differential equations and solved using collocation method via the bvp4c in MATLAB. It is found that the nanoparticle volume fraction reduces the velocity of the fluid for silver nanoparticle in the case of divergent channel. For a convergent, the increase in the volume fraction increases the velocity. Stretching divergent channel increases the flow near the walls of the channel. Shrinking convergent channel reduces the velocity of the fluid near the walls of the channel. The Grashof number increases the temperature in divergent channel and reduces the temperature in convergent channel. The Eckert number increases temperature of the fluid for all the cases. The heat generation parameter increases the velocity and temperature for both convergent and divergent channel. The heat generation parameter decreases the concentration of Nanofluid flow for both divergent and convergent. This kind of Nanofluid flow has a variety of applications such as the transportation of chemotherapy drug directly to cancerous growth as well as to deliver drugs to areas of arteries that are damaged in order to fight cardiovascular diseases.

Keywords: Unsteadiness, MHD Nanofluid Flow, Heat and Mass Transfer, Divergent-Convergent Channel

1. Introduction

Magneto hydrodynamics is the study of interaction of electrical conducting fluids and electromagnetic forces. The field of MHD was initiated by Swedish Physicist, Hannes Alves [1].

Hartmann [2] investigated the influence of transverse uniform magnetic field on the flow of viscous incompressible electrically conducting fluid between two infinite parallel stationary and insulating plates. Nanotechnology has assisted in engineering and bio-medical sciences.

Elli [3] investigated the magneto hydrodynamic flow of non-Newtonian Nanofluid in pipe. He discovered that MHD parameter decreases the fluid motion and the velocity profile is larger than that of temperature profile even in the presence of variable viscosity.

Makinde [4] investigated the effects of buoyancy force convective heating, Brownian motion, thermophoresis and magnetic field on stagnation point flow and heat transfer due to Nanofluid flow towards a stretching sheet. He found that there exists dual solution for shrinking case. The skin coefficient and the local Sherwood number decrease while the local Nusselt number increases with increasing intensity of buoyancy force. A large number of Nanoparticle drug delivery system have been developed for cancer treatment and various nanomaterials have been explored as drug delivery agents to improve the therapeutic efficacy and safety of anticancer drug [5]. Nanoparticle is small particle that ranges between 1 to 100 Nano metres. Most Nanoparticles are made up of a few hundred atoms [6].

During the circulation, the blood carries the heat transfer

coefficient of the blood, the density of the blood flow, the velocity of the blood flow, radius of the artery and temperature of the tissues that surround the artery [7]. The importance of radioactive heat transfer in blood vessels, the radiation effect in blood is of great importance to bio-medical experts in the therapeutic procedure of hyperthermia, which has a well-recognized in oncology. Its effects are attained by overheating the cancerous tissues by means of electromagnetic radiation [8].

Mburu [9] investigated magneto hydrodynamic Nanofluid flow through converging-divergent channel under weak magnetic field. They found that the nanoparticle volume fraction increases the thermal transportation of the fluid without affecting its velocity profiles. They observed that as the channel converges there is a pressure decrease but as the fluid passes through the throat of the converging-diverging channel the pressure increases.

Muhammad [10] studied a fluid flow and heat transfer of blood with nanoparticle through porous vessels in the presence of magnetic field. The blood flow is assumed to be non-Newtonian and collocation and least squares techniques were used and they found that the thermophoresis and Brownian movement perform an essential part on the temperature and Nanoparticles focus conveyance.

Virginia [11] did control volume analysis of MHD flow of Nanoparticles as results of stretching surface and suction. It was found that the velocity profiles decrease when Nanoparticle volume fraction increases, temperature profiles increase with addition of amount of Nanoparticles. Increased in temperature is caused by slow movement of particles which increase thermal conductivity. It was discovered that the concentration profiles decrease when Nanoparticle fraction increases and when the stretching parameter is increased the velocity profiles of the Nanofluid increase.

Onyango [12] carried out a study on heat and mass transfer of MHD Jeffrey-Hammel flow in the presence of inclined magnetic field. They found that the temperature profiles increase with the increase in the suction parameter, Eckert number, Grashof temperature number, Hartmann number, wedge angle and Prandtl number but decrease with the increase with the injection parameter. The concentration of the fluid increases with the increase in the unsteadiness parameter and the angle parameter. Magnetic induction and velocity increase with the increase in the Grashof temperature and concentration numbers. The temperature decreases with time while the magnetic induction increases with the increase in the Reynolds number.

Nidal [13] did investigation on controlled drug delivery using the magnetic Nanoparticle in non-Newtonian blood vessels. They numerically examined the movement of magnetic nanoparticles in the non- Newtonian blood vessels under the influence of magnetic field. The magnetic field was applied perpendicular to the direction of the transport of nanoparticles. They discovered that considering non-Newtonian parameter of the fluid was crucial.

Ashish Mishra [14] investigated the roles of Nanoparticles and heat generation/absorption on MHD flow of Silver-water via porous stretching/shrinking converging/diverging. The results show that the thermal boundary layer thickness of the stretching/diverging and shrinking/converging channel enhance by increasing the value of Eckert number while the opposite tendency is scrutinized on the momentum boundary layer thickness by increasing the value of porosity parameter for the stretching /diverging and the shrinking /converging channel.

For the best knowledge of the researcher, the effect of heat and mass transfer on unsteady MHD Nanofluid flow through converging-diverging channel is new area of interest for study.

The study is aimed at developing governing equations, determining the effects of Nanoparticle volume fractions, heat and mass transfer, unsteadiness time parameter, heat generation parameter, Eckert number on velocity, temperature and concentration of unsteady MHD Nanofluid flow through convergent-divergent channel.

2. The Effect of Heat and Mass Transfer on Unsteady MHD Nanofluid Flow

2.1. Nomenclature (Abbreviation)

γ : Unsteadiness Time Parameter
λ : Heat Generation Parameter
Ψ : Volume Fraction of Nanoparticles
Ag: Silver
B_0: Magnetic Field
D_m: Concentration Mass Diffusivity
D_f: Dufour Number
E_c: Eckert Number
G_r: Grashof Number
Ha: Hartmann Number
K: Thermal Conductivity
K_{nf}: Nanofluid Thermal Conductivity
K_T: Thermal Diffusion Ratio
Re: Reynolds Number
S_c: Schmidt Number
MHD: Magnetohydrodynamics

2.2. Mathematical Formulation

In this paper, we consider unsteady two dimensional MHD Nanofluid flow in convergent- divergent channel. The velocity of the Nanofluid is given by

$$\vec{q} = \vec{q}(r, \theta, t) \tag{1}$$

When the angle of the channel is greater (less) than $\alpha > 0 (\alpha < 0)$ the channel will be divergent (convergent).

From Figure 1. The fluid flow is two dimensional, incompressible, at the walls the temperature and concentration of Nanofluid are constants. At the centre the velocity is maximum. The temperature and concentration of Nanofluid far away from the walls are maximum. The temperature and concentration differences in the Nanofluid flow give rise to buoyancy forces. The equations governing the effect of heat and mass transfer of an unsteady MHD

Nanofluid flow in the cylindrical coordinates are: conservation of the mass, momentum equation, energy equation and concentration equation. We outline these equations as follows;

$$\rho_{nf}\left[\frac{1}{r}\frac{\partial}{\partial r}(rq_r)+\frac{1}{r}\frac{\partial}{\partial\theta}(q_\theta)+\frac{\partial}{\partial z}(q_z)\right]=0 \tag{2}$$

$$\frac{\partial^2 q_r}{\partial t\partial\theta}+\frac{\partial q_r}{\partial\theta}\cdot\frac{\partial q_r}{\partial r}+q_r\frac{\partial^2 q_r}{\partial\theta\partial r}+\frac{q_\theta}{r}\left(\frac{\partial^2 q_r}{\partial\theta^2}\right)-q_\theta\frac{\partial q_r}{\partial r}=\frac{\mu_{nf}}{\rho_{nf}}\left[\frac{1}{r}\frac{\partial}{\partial\theta}\left(\frac{\partial q_r}{\partial r}\right)+\frac{\partial}{\partial\theta}\left(\frac{\partial^2 q_r}{\partial r^2}\right)-\frac{q_r}{r^2}+\frac{1}{r^2}\left(\frac{\partial^3 q_r}{\partial\theta^3}\right)-\frac{q_\theta}{r^2}+\frac{2}{r^2}\frac{\partial q_r}{\partial\theta}-\frac{2}{r}\frac{\partial}{\partial r}\left(\frac{\partial q_r}{\partial\theta}\right)\right]+\frac{\sigma_{nf}}{\rho_{nf}}\frac{\partial}{\partial\theta}\left(\frac{B_0}{r}q_\theta-\frac{B^2{}_0}{r^2}q_r\right)-g_{nf}[\beta_T(T-T_\infty)+\beta_C(C-C_\infty)]-\frac{\sigma_{nf}}{\rho_{nf}}\frac{\partial}{\partial r}\left(b\frac{B_0}{r}q_r-b^2q_\theta\right) \tag{3}$$

$$\frac{\partial T}{\partial t}+q_r\frac{\partial T}{\partial r}+q_\theta\frac{\partial T}{\partial\theta}=\frac{K_{nf}}{(\rho C_P)_{nf}}\left[\frac{1}{r}\frac{\partial}{\partial r}\left(r\frac{\partial T}{\partial r}\right)+\frac{1}{r^2}\left(\frac{\partial^2 T}{\partial\theta^2}\right)\right]+\frac{K_T}{(\rho C_P)}\left[\frac{1}{r}\frac{\partial}{\partial r}\left(r\frac{\partial C}{\partial r}\right)+\frac{1}{r^2}\left(\frac{\partial^2 C}{\partial\theta^2}\right)\right]+\frac{\mu_{nf}}{(\rho C_P)_{nf}}\left[2\left(\frac{\partial q_r}{\partial r}\right)^2+2\left(\frac{q_r}{r}\right)^2+\left(-\frac{q_\theta}{r}+\frac{1}{r}\frac{\partial q_r}{\partial\theta}\right)^2\right]+\frac{1}{(\rho C_P)_{nf}}\left[\frac{Q_0T}{r^2}+\sigma_{nf}\left(\frac{B_0}{r}q_\theta-\frac{B^2{}_0}{r^2}q_r\right)+\sigma_{nf}\left(\frac{B_0}{r}bq_r-b^2q_\theta\right)\right] \tag{4}$$

$$\frac{\partial C}{\partial t}+q_r\frac{\partial C}{\partial r}+q_\theta\frac{\partial C}{\partial\theta}=D_B\left[\frac{1}{r}\frac{\partial}{\partial r}\left(r\frac{\partial C}{\partial r}\right)+\frac{1}{r^2}\left(\frac{\partial^2 C}{\partial\theta^2}\right)\right]+D_T\left[\frac{1}{r}\frac{\partial}{\partial r}\left(r\frac{\partial T}{\partial r}\right)+\frac{1}{r^2}\left(\frac{\partial^2 T}{\partial\theta^2}\right)\right]+R\nabla(C-C_\infty) \tag{5}$$

2.3. Thermophysical Characteristics

Nanofluid enhances the effectiveness of heat transfer fluids. Thermo-physical properties of the Nanofluids are essential for determination of the heat transfer behavior. For instance, the thermal conductivity of Nanofluids depends on particle volume fraction, particle material, particle size, base fluid material and temperature. In this study we considered the following Thermophysical characteristics of silver-water Nanoparticles [15]. Table 1.

In this paper, we consider the MHD Nanofluid flow, the walls of the channel make an angle θ between them. The angle becomes maximum when $\theta=2\alpha$ so that α represents the upper wall and $-\alpha$ for lower wall. That is $-\alpha\le\theta\le\alpha$. The boundary conditions for Nanofluid flow are given below

$$q_r=0, q_\theta=v_0, T=T_w, C=C_w \text{ at } \theta=\pm\alpha$$

$$q_r=Q, q_\theta=0, T=T_\infty, C=C_\infty \text{ at } \theta=0$$

Where T_w and T_∞ are wall and free stream temperatures respectively. Q, C_w and C_∞ are free stream velocity, wall and free stream concentrations respectively.

2.4. Thermal Conductivity and Viscosity of the Nanofluid

Einstein [16] discovered the effective viscosity of suspension of spherical solids as a function of volume fraction using the phenomenological hydrodynamic equations. Brinkman [17] discussed a viscosity correlation equation of suspensions with moderate particle volume fraction, typically less than 4 percent. Xuan and Roetzel [18] explain the density of the Nanofluids as a function of the particle volume concentration and show the density of the base fluid and the specific heat at constant pressure.

$$K_{nf}=\left(\frac{K_s+2K_f+2\psi(K_f-K_s)}{K_s+2K_f+\psi(K_s-K_f)}\right)K_f \tag{6}$$

$$\frac{\mu_{nf}}{\mu_f}=\frac{1}{(1-\psi)^{2.5}} \tag{7}$$

$$\rho_{nf}=(1-\psi)\rho_s+\psi\rho_f \tag{8}$$

$$(\rho C_P)_{nf}=(1-\psi)(\rho C_P)_f+\psi(\rho C_P)_s \tag{9}$$

2.5. Similarity Transformation of Specific Equations

2.5.1. Similarity Transformation Relation

Similarity transformation is applied to reduce the governing non-linear differential equations (3), (4) and (5) into ordinary differential equations. The relations for similarity transformation of velocities are expressed as follows;

$$q_r(r,\theta,t)=\frac{Qf(\eta)}{r\delta^{m+1}} \tag{10}$$

$$q_\theta(r,\theta,t)=\frac{Qg(\eta)}{r\delta^{m+1}} \tag{11}$$

While those of temperature and concentration are expressed as

$$\frac{\phi(\eta)}{\delta^{m+1}}=\frac{T-T_\infty}{T_w-T_\infty} \tag{12}$$

$$\frac{\psi(\eta)}{\delta^{m+1}}=\frac{C-C_\infty}{C_w-C_\infty} \tag{13}$$

Where

$$\eta=\frac{\theta}{\alpha} \tag{14}$$

2.5.2. Transformation of Governing Equations

To transform the governing equations, relations (10) to (14) are used. We start by showing the conservation law is satisfied, that is;

$$\rho_{nf}\left(\frac{1}{r}\frac{\partial}{\partial r}(rq_r)\right)=\rho_{nf}\left(-\frac{Q}{r^2\delta^{m+1}}f+\frac{Q}{r^2\delta^{m+1}}f\right)=0 \tag{15}$$

Using (10), (11) in (3) yields

$$-(m+1)\left(\frac{r^{m+1}\alpha^2}{\delta^{m+1}}\gamma f'\right)-\frac{2\alpha^2}{r\delta^{m+1}}ReA_1(1-\psi)^{-2.5}v_f ff'+\alpha\frac{v_0}{Q}Re(f''+\alpha f)=\left(5\alpha^2-\frac{\alpha^2}{r^2}(Ha)^2\right)f'+f'''+\left(\alpha^3-\frac{2\alpha^3}{r}\right)f+\alpha^3v_0+Ha\sqrt{\frac{\sigma_{nf}}{\mu_{nf}}}\frac{Q\alpha^2}{r\delta^{m+1}}\left[\omega f'+f\omega'+\frac{3\alpha}{r}\omega f\right]-(Ha)^2\frac{\alpha^2}{r^2}f'-\frac{\sigma_{nf}}{\mu_{nf}}\frac{2Qv_0\alpha^3}{\delta^{m+1}}\omega^2+\alpha^3G_r(T)\phi+\alpha^3G_r(C)\psi \tag{16}$$

Using (10), (11), (12) and (13) in (4) yields

$$-\frac{(m+1)r^{m+1}\alpha^2}{\delta^{m+1}}\gamma P_r\phi+\alpha\frac{A_2}{A_3}v_0P_r\phi'=\phi''+D_fP_r\psi''+E_cP_r\left[4\frac{\alpha^2}{\delta^{m+1}}f^2+\frac{r^2}{Q^2}\alpha^2(v_0)^2-2\frac{r^2}{Q}v_0\alpha f'+\frac{1}{\delta^{m+1}}(f')^2\right]+r^2\alpha^2E_cP_r\lambda\phi-\frac{\alpha^2}{rQ}(1-\psi)^{2.5}\mu_f(Ha)^2E_cP_rf+\frac{\alpha^2}{Q}(1-\psi)^{2.5}\mu_f\sqrt{\frac{\sigma_{nf}}{\mu_{nf}}}HaE_cP_rf\omega \quad (17)$$

Using (12), (13) in (5) yields

$$\frac{-(m+1)r^{m+1}}{\delta^{m+1}}\alpha^2S_c\gamma\psi+\frac{Q\alpha r}{\delta^{m+1}}A_1(1-\psi)^{-2.5}v_0S_c\psi'=\psi''+S_cS_r\phi''+\frac{RS_cRe\alpha}{Q}\psi' \quad (18)$$

Where the Schmidt number is represented by $S_c=\frac{\nu}{D}$, the Soret number is $S_r=\frac{D_T(T_w-T_\infty)}{\nu(C_w-C_\infty)}$, the Reynolds number is defined by $R_e=\frac{rQ}{\nu}$, the Hartmann is defined by $(Ha)^2=\frac{\sigma_{nf}}{\mu_{nf}}r^2(B_0)^2$, the Grashof number for temperature and concentration is defined by $G_r(T)=\frac{gr^3\beta_T}{\nu Q}(T_w-T_\infty)$, $G_r(C)=\frac{gr^3\beta_C}{\nu Q}(C_w-C_\infty)$, the Prandtl number is defined as $P_r=\frac{\mu C_P}{K}$, Eckert number is represented as $E_c=\frac{Q^2}{r^2C_P(T_w-T_\infty)}$, the heat generation parameter is defined as $\lambda=\frac{Q_0(T_w-T_\infty)}{Q^2}$, the Dufour number is defined as $D_f=\frac{K_T(C_w-C_\infty)}{\mu C_P(T_w-T_\infty)}$, the unsteadiness time parameter is defined as $\gamma=\frac{\delta^m}{\nu r^{m-1}}\delta'$, $A_1=\left[\psi\left(\frac{\rho_s}{\rho_f}\right)+(1-\psi)\right]$, $A_2=\left[\psi\left(\frac{(\rho C_P)_s}{(\rho C_P)_f}\right)+(1-\psi)\right]$, $A_3=\left(\frac{K_s+2K_f+2\psi(K_f-K_s)}{K_s+2K_f+\psi(K_s-K_f)}\right)$,

$$A_4=\left[\psi\left(\frac{\sigma_s}{\sigma_f}\right)+(1-\psi)\right],g=v_0$$

$$\eta\to 0: f=\frac{f_r\,r}{Q}\delta^{m+1},\phi=0,\psi=0,f'=0,\phi'=0,\psi'=0$$

$$\eta\to\infty: f=0,\phi=\delta^{m+1},\psi=\delta^{m+1},f'=1,\phi'=1,\psi'=1$$

2.6. Numerical Method

The laminar two- dimensional unsteady MHD Nanofluid flow in the convergent-divergent channel is studied. The collocation method is a method for numerical solution of the ordinary differential equations. In this method a finite dimensional space of solutions and a number of points in the domain known as collocation points and the solution is evaluated at the collocation points by integration of a system of differential equations of the form.

$$z'=F(\eta,z) \quad (19)$$

Specified by ordinary differential equation function, subject to the boundary conditions described by the boundary condition function and the initial solution guess. Equations (16), (17) and (18) are re-written as

The transformed boundary conditions are as follows;

$$f'''=-(m+1)\left(\frac{r^{m+1}\alpha^2}{\delta^{m+1}}\gamma f'\right)-\frac{2\alpha^2}{r\delta^{m+1}}ReA_1(1-\psi)^{-2.5}v_ff f''+\alpha\frac{v_0}{Q}Re(f''+\alpha f)-\left(5\alpha^2-\frac{\alpha^2}{r^2}(Ha)^2\right)f'-\left(\alpha^3-\frac{2\alpha^3}{r}\right)f-\alpha^3v_0-\alpha^3G_r(T)\phi-\alpha^3G_r(C)\psi-Ha\sqrt{\frac{\sigma_{nf}}{\mu_{nf}}}\frac{Q\alpha^2}{r\delta^{m+1}}\left[\omega f'+f\omega'+\frac{3\alpha}{r}\omega f\right]+(Ha)^2\frac{\alpha^2}{r^2}f'+\frac{\sigma_{nf}}{\mu_{nf}}\frac{2Qv_0\alpha^3}{\delta^{m+1}}\omega^2 \quad (20)$$

$$\phi''=-\frac{(m+1)r^{m+1}\alpha^2}{\delta^{m+1}}\gamma P_r\phi+\alpha\frac{A_2}{A_3}v_0P_r\phi'-D_fP_r\psi''-E_cP_r\left[4\frac{\alpha^2}{\delta^{m+1}}f^2+\frac{r^2}{Q^2}\alpha^2(v_0)^2-2\frac{r^2}{Q}v_0\alpha f'+\frac{1}{\delta^{m+1}}(f')^2\right]-r^2\alpha^2E_cP_r\lambda\phi+\frac{\alpha^2}{rQ}(1-\psi)^{2.5}\mu_f(Ha)^2E_cP_rf-\frac{\alpha^2}{Q}(1-\psi)^{2.5}\mu_f\sqrt{\frac{\sigma_{nf}}{\mu_{nf}}}HaE_cP_rf\omega. \quad (21)$$

$$\psi''=\frac{-(m+1)r^{m+1}}{\delta^{m+1}}\alpha^2S_c\gamma\psi+\frac{Q\alpha r}{\delta^{m+1}}A_1(1-\psi)^{-2.5}v_0S_c\psi'-S_cS_r\phi''-\frac{RS_cRe\alpha}{Q}\psi' \quad (22)$$

Equations (20),(21) and (22) are higher order of non-linear ordinary differential equations and to get the numerical simulations, the higher orders are reduced to first order ordinary differential equations to achieve (32) by letting

$$z_1=f;z_2=f';z_3=f'';z_4=\phi;z_5=\phi';z_6=\psi;z_7=\psi' \quad (23)$$

From equation (23), we get

$$z'_1=z_2 \quad (24)$$

$$z'_2=z_3 \quad (25)$$

$$z'_3=f'''=-(m+1)\left(\frac{r^{m+1}\alpha^2}{\delta^{m+1}}\gamma\right)z_2-\frac{2\alpha^2}{r\delta^{m+1}}ReA_1(1-\psi)^{-2.5}v_fz_1z_2+\alpha\frac{v_0}{Q}Re(z_3+\alpha z_1)-\left(5\alpha^2-\frac{\alpha^2}{r^2}(Ha)^2\right)z_2-\left(\alpha^3-\frac{2\alpha^3}{r}\right)z_1-\alpha^3v_0-\alpha^3G_r(T)z_4-\alpha^3G_r(C)z_6-Ha\sqrt{\frac{\sigma_{nf}}{\mu_{nf}}}\frac{Q\alpha^2}{r\delta^{m+1}}\left[z_8z_2+z_1z_9+\frac{3\alpha}{r}z_8z_1\right]+(Ha)^2\frac{\alpha^2}{r^2}z_2+\frac{\sigma_{nf}}{\mu_{nf}}\frac{2Qv_0\alpha^3}{\delta^{m+1}}(z_8)^2:U \quad (26)$$

$$z'_4 = z_5 \tag{27}$$

$$z'_5 = \phi'' = -\frac{(m+1)r^{m+1}\alpha^2}{\delta^{m+1}}\gamma P_r z_4 + \alpha\frac{A_2}{A_3}v_0 P_r z_5 - D_f P_r z'_7 - E_c P_r\left[4\frac{\alpha^2}{\delta^{m+1}}(z_1)^2 + \frac{r^2}{Q^2}\alpha^2(v_0)^2 - 2\frac{r^2}{Q}v_0\alpha z_2 + \frac{1}{\delta^{m+1}}(z_2)^2\right] - r^2\alpha^2 E_c P_r\lambda z_4 + \frac{\alpha^2}{rQ}(1-\psi)^{2.5}\mu_f(Ha)^2 E_c P_r z_1 - \frac{\alpha^2}{Q}(1-\psi)^{2.5}\mu_f\sqrt{\frac{\sigma_{nf}}{\mu_{nf}}}HaE_c P_r z_1 z_8 : V \tag{28}$$

$$z'_6 = z_7 \tag{29}$$

$$z'_7 = \psi'' = \frac{-(m+1)r^{m+1}}{\delta^{m+1}}\alpha^2 S_c\gamma z_6 + \frac{Q\alpha r}{\delta^{m+1}}A_1(1-\psi)^{-2.5}v_0 S_c z_7 - S_c S_r z'_5 - \frac{RS_c Re\alpha}{Q}z_7 : W \tag{30}$$

$$z'_8 = z_9 \tag{31}$$

The equations (24) to (31) yield the following systems of equations.

$$z' = F(\eta, z) \tag{32}$$

$$z = \begin{pmatrix} z_1 \\ z_2 \\ z_3 \\ z_4 \\ z_5 \\ z_6 \\ z_7 \\ z_8 \end{pmatrix} \quad F = \begin{pmatrix} z_2 \\ z_3 \\ U \\ z_5 \\ V \\ z_7 \\ W \\ z_9 \end{pmatrix} \tag{33}$$

3. Results and Discussion

Table 1. *Thermophysical Characteristics of Silver and Water.*

Nanoparticles	C_P	K	ρ	σ
Water	997.1	4179	0.613	0.06
Silver	10500	235	4291	6.3×10^7

Table 2. *Values of Physical Parameters.*

Re	G_r	E_c	γ	λ	ψ
15	5	0.02	0	0	0.2
20	20	0.06	0.5	2	0.5
25	35	0.1	1	5	0.7

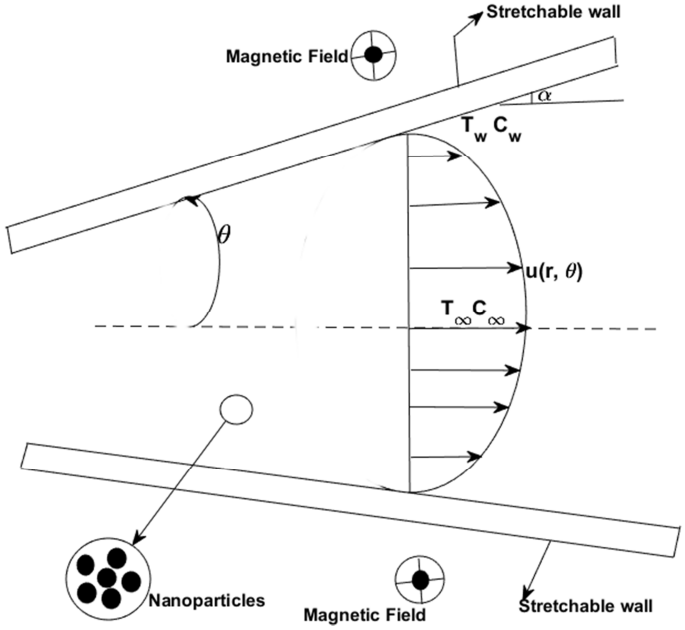

Figure 1. *Flow Diagram of Unsteady MHD Nanofluid Flow Through convergent-Divergent Channel with Heat and Mass Transfer.*

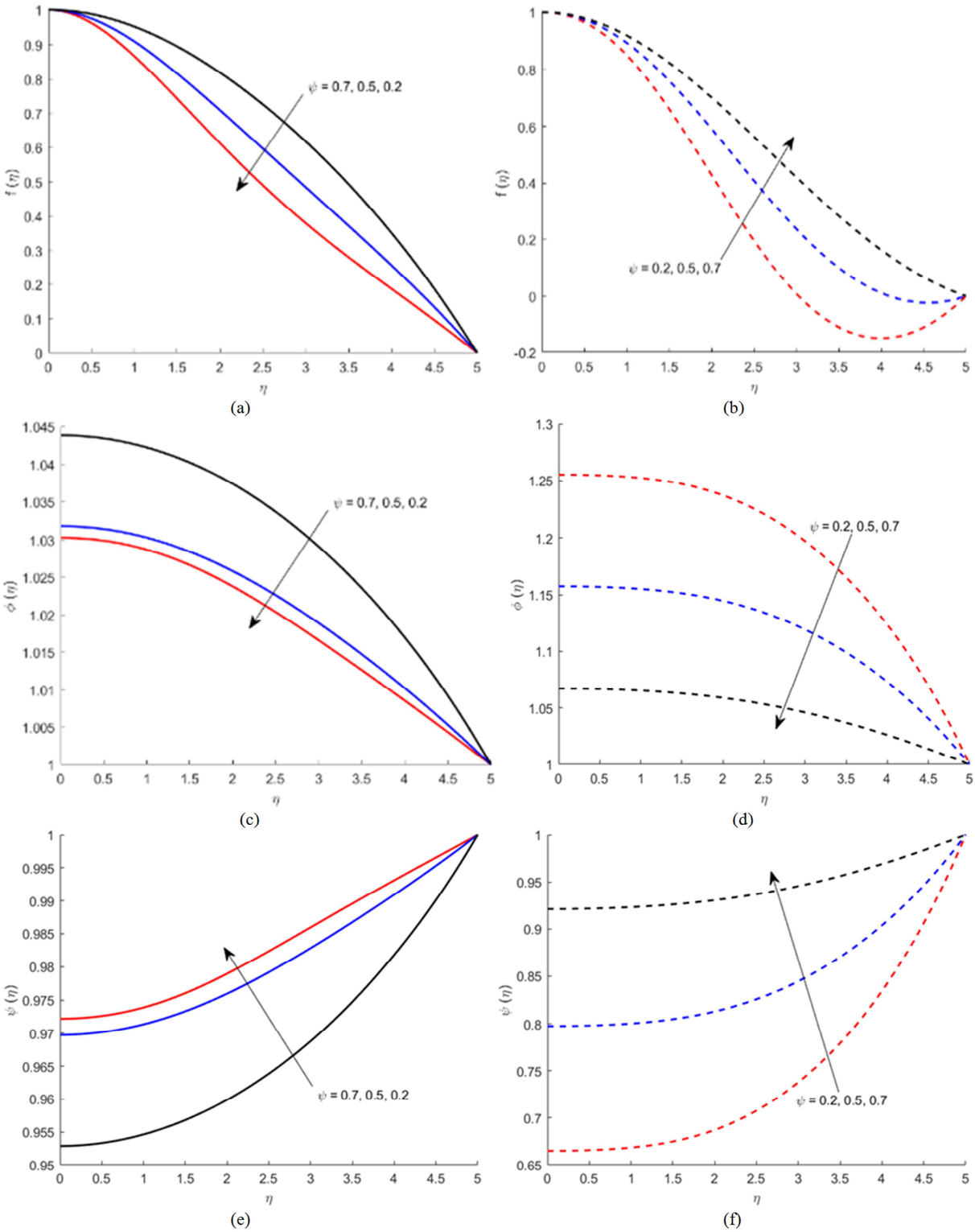

Figure 2. *Effect of nanoparticle volume fraction on velocity* $(f(\eta))$*, temperature* $(\phi(\eta))$ *and concentration* $(\psi(\eta))$ *profiles for a divergent (Left panel) and a convergent (Right panel) channel.*

We present the results of parameters variations (Unsteadiness time parameter, the Eckert number, Reynolds number, Grashof number, heat generation parameter) and effects of nanoparticle volume fraction on the velocity, temperature and concentration profiles. The Prandtl number is fixed as 6.2 due the base fluid that is water. The different values of physical parameters are given in the table 2 that are used to generate the Graphs**.** Results and discussions on unsteady MHD Nanofluid flow are presented below. The divergent channel is represented by solid lines and convergent channel is represented by dashed line.

Studies on MHD Nanofluid Flow through convergent-

divergent channel have been done before. Ashish Mishra [14] carried out a study on the roles of Nanoparticle and heat generation/absorption on MHD via porous stretching/shrinking convergent/divergent channel. They determined the effect of nanoparticle volume fraction, Hartmann number, Grashof number, Eckert number, Heat generation parameter, Reynolds number on velocity and temperature profiles. In the current study, a researcher contributes on the effect of the unsteadiness time parameter and extends the investigation on the mass transfer of the Nanofluid flow that were not considered in the previous study.

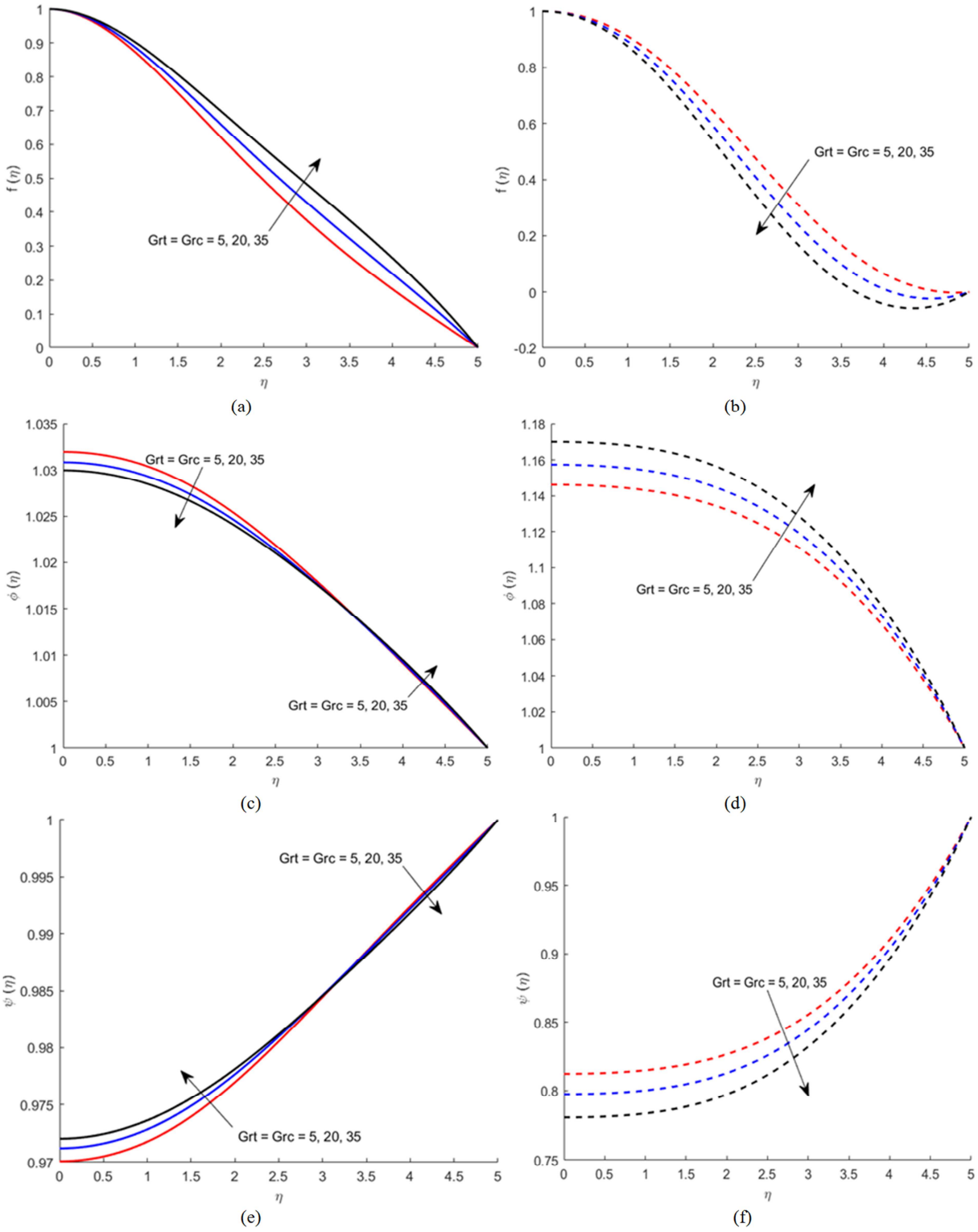

Figure 3. *Effect of Grashof number on velocity* $(f(\eta))$*, temperature* $(\phi(\eta))$ *and concentration* $(\psi(\eta))$ *profiles for a divergent (Left panel) and a convergent (Right panel) channel.*

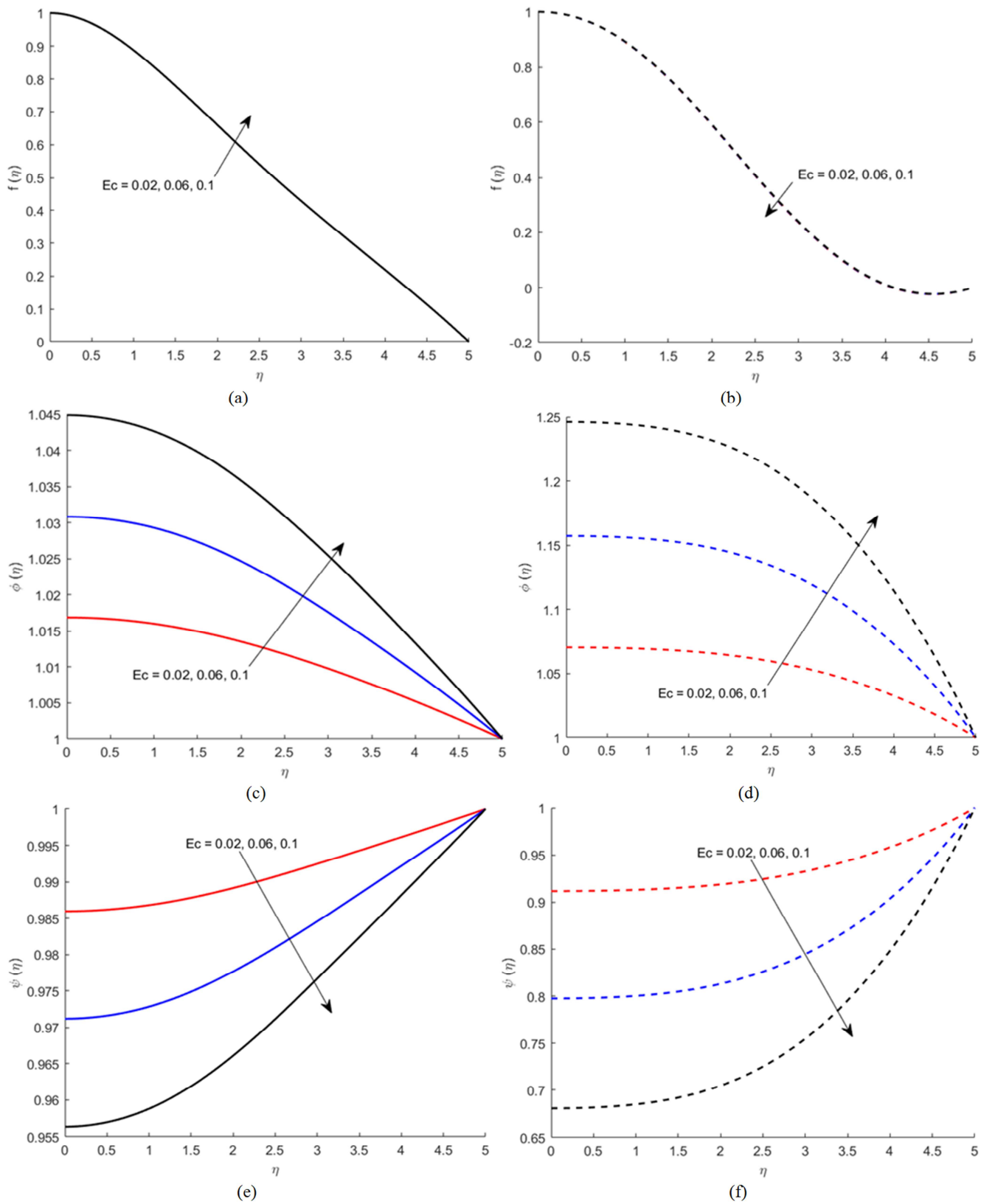

Figure 4. *Effect of Eckert number on velocity* $(f(\eta))$*, temperature* $(\phi(\eta))$ *and concentration* $(\psi(\eta))$ *profiles for a divergent (Left panel) and a convergent (Right panel) channel.*

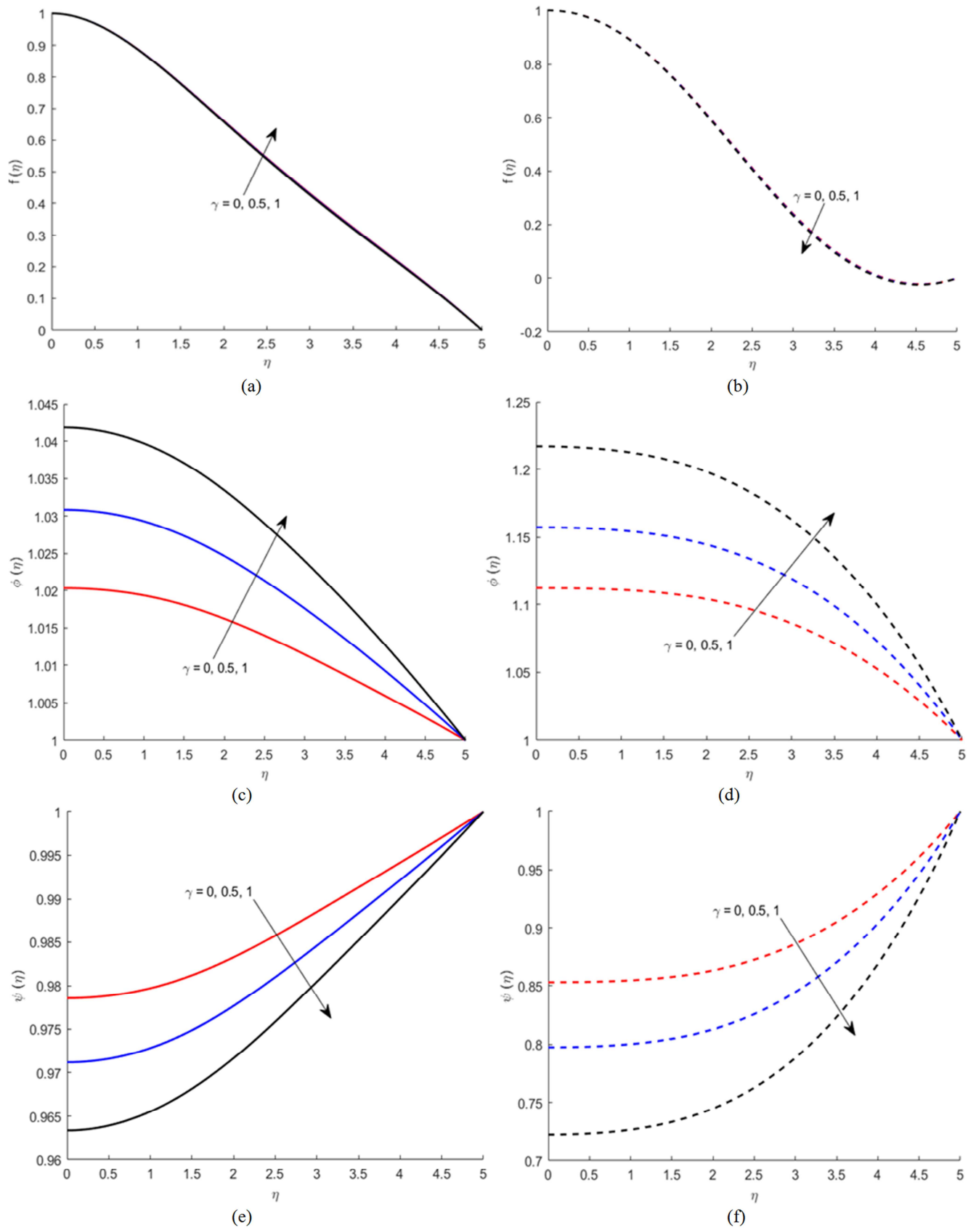

Figure 5. *Effect of unsteadiness time parameter on velocity* $(f(\eta))$*, temperature* $(\phi(\eta))$ *and concentration* $(\psi(\eta))$ *profiles for a divergent (Left panel) and a convergent (Right panel) channel.*

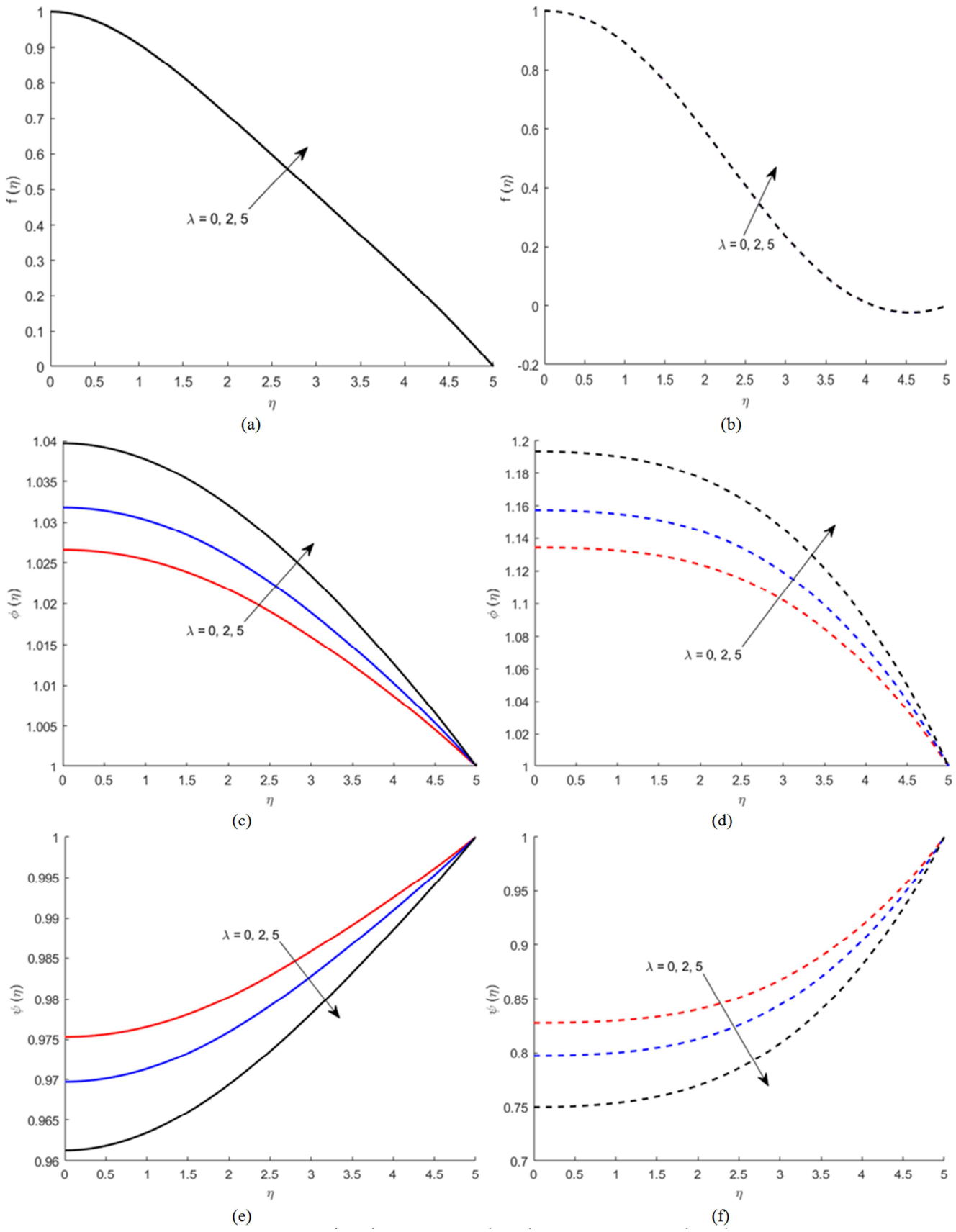

Figure 6. *Effect of heat generation parameter on velocity* $(f(\eta))$*, temperature* $(\phi(\eta))$ *and concentration* $(\psi(\eta))$ *profiles for a divergent (Left panel) and a convergent (Right panel) channel.*

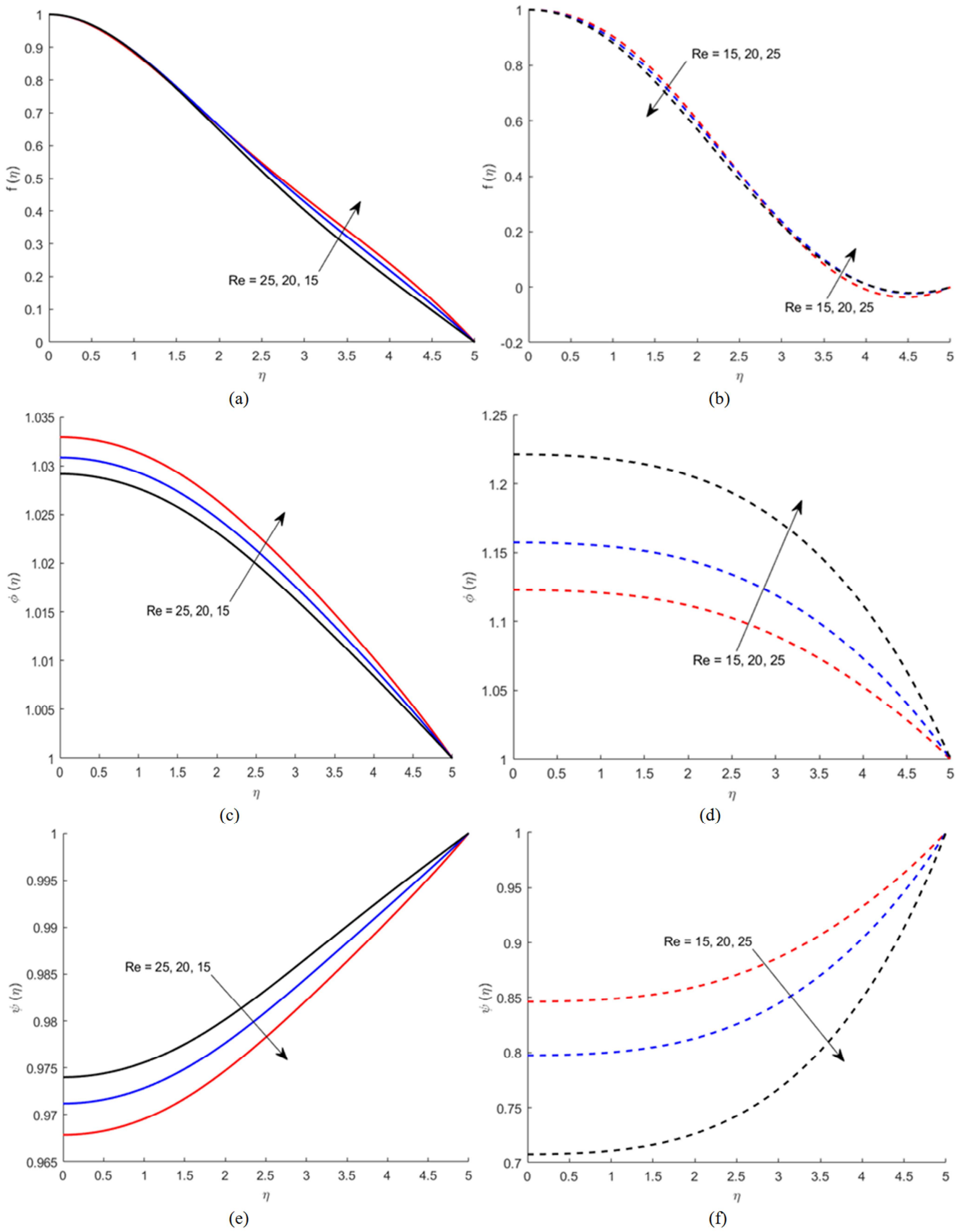

Figure 7. *Effect of Reynolds number on velocity* $(f(\eta))$*, temperature* $(\phi(\eta))$ *and concentration* $(\psi(\eta))$ *profiles for a divergent (Left panel) and a convergent (Right panel) channel.*

From Figure 2(a). The velocity of the Nanofluid decreases with the increase in the nanoparticle volume fraction.

Viscous effects can be considered as responsible for this result. From Figure 2(b). The rise in temperature due to thermal conductivity of the nanoparticles reduces the effect of viscous drag force hence increased velocity. From Figure 2(c) and 2(d). The reduction in the temperature is due to the fact that the thermal conductivity and thermal boundary layer thickness decreases with the increasing values of the nanoparticle volume fraction. From Figure 2(e) and 2(f). The concentration of the Nanofluid increases with the increase in the nanoparticle volume fraction. As nanoparticle volume fraction increases, the thermal conductivity and thermal boundary layer thickness reduce which in turn leads to low kinetic energy that reduces the distance between the Nanofluid molecules hence increased concentration.

From Figure 3(a). The increase in the Grashof number leads to a decrease of the viscous forces and this reduces the effect of the drag forces in the Nanofluid flow; hence the increased velocity. From Figure 3(b). The velocity decreases with the increase in the Grashof number. This is due to the effect of viscous forces that increases the drag forces which lead to reduction of velocity. From Figure 3(c) and 3(d). The increase in the values of the Grashof number leads to the rise in temperature due to the fact that the viscosity and temperature have the inverse relationship, then the temperature increases when the viscous forces decrease. From Figure 3(e) and 3(f). The concentration of the Nanofluid decreases with the increase in the Grashof number. This is due to the rise in temperature that causes the increase in the kinetic energy which in turn leads to the increase in the space between the molecules of Nanofluid then resulting in decreased concentration.

From Figure 4(a). The Eckert number denotes the effect of viscous dissipation on thermal field. When the Eckert number increases, the Nanofluid friction plays dominant role to increase the amount of heat and Nanofluid flow rate along the maximum point of the channel becomes faster, hence increased velocity. From Figure 4(b). The velocity decreases with the increase in the Eckert number. This is due to the thickness of the thermal boundary layer, hence reduced velocity. From Figure 4(c) and 4(d). The temperature of the Nanofluid increases with the increase in the Eckert number. The rise in temperature is due to stronger viscous dissipation in both channel. From Figure 4(e) and 4(f). The concentration of the Nanofluid decreases with the increase in the Eckert number. As the values of Eckert number increase, the temperature will rise and the kinetic energy increases, which lead to the increase in the space between the Nanofluid molecules, hence the reduction in concentration on the Nanofluid in both channel.

From Figure 5(a). The velocity increases with the increase in the unsteadiness time parameter. The increase in the unsteadiness time parameter leads to widening of the boundary layer thickness, hence increased velocity. From Figure 5(b). The velocity decreases with the increase in the unsteadiness time parameter. The boundary layer is reduced due to no-slip condition and viscous drag forces which leads to the decreased velocity. From Figure 5(c) and 5(d). The temperature increases with the increase in the unsteadiness time parameter, this is due to the fact that viscosity and temperature are inversely related. A decrease of viscous forces leads to an increase in temperature. From Figure 5(e) and 5(f). The concentration of Nanofluid decreases with the increase in the unsteadiness time parameter due to the mass diffusion within the concentration boundary layer region.

From Figure 6(a) and 6(b). The velocity increases at constant speed with the increase in the heat generation parameter. This is due to the rise in the temperature that reduces the viscous forces. From Figure 6(c) and 6(d). The temperature of the Nanofluid increases with the increase in the heat generation parameter due to the widening of the thermal boundary layer, the heat generation increases the heat transfer and the maximum amount of heat leads to rise in temperature. From Figure 6(e) and 6(f). The concentration of Nanofluid decreases with the increases in the heat generation parameter. The rise in temperature leads to an increase in the energy that widen the distance between Nanofluid molecules hence reduction in concentration of Nanofluid.

From Figure 7(a). The velocity increases with the increase in the Reynolds number. The viscous drag force is reduced as the viscous forces decreases hence increased velocity. From Figure 7(b). The velocity increases with the increase in the Reynolds number. This is due to the effect of viscous force. From Figure 7(c) and 7(d). The temperature profiles increase with the increase in the Reynolds number. This is due to the fact that viscosity and temperature have inverse relationship, then a reduction in viscous forces lead to rise in temperature in both convergent-divergent channel.

From Figure 7(e) and 7(f). The concentration decreases with the increase in the Reynolds number. The rise in temperature is associated to the rise in the kinetic energy of the Nanofluid which enlarges the distance between the molecules that leads to reduction in concentration.

4. Conclusion

1) The nanoparticle volume fraction decreases the velocity of the Nanofluid in the case of divergent channel. For a convergent channel, the increase in the volume fraction increases the velocity. Temperature decreases for increasing the values of nanoparticle volume fraction for both stretching and shrinking channels. The higher amount of nanoparticle volume fraction, higher value in the concentration of Nanofluid for both divergent and convergent channel.
2) The Grashof number increases the velocity in divergent channel due to temperature differences and reduces the velocity in convergent channel due to viscous forces. The Grashof number decreases the temperature in divergent channel and increases the temperature in convergent channel. The Grashof number increases the concentration from the walls to the centre and reduces the concentration at center line in divergent channel. It decreases the concentration.
3) Eckert number increases temperature of the Nanofluid for all the cases. The unsteadiness time parameter

increases the velocity in divergent channel and decreases the velocity in convergent channel. It increases the temperature for both divergent and convergent channel. The concentration of Nanofluid decreases with the increase in the unsteadiness time parameter for both divergent and convergent channel.

4) The heat generation parameter increases the velocity and temperature for both divergent and convergent channel. The heat generation decreases the concentration of Nanofluid for both divergent and convergent channel.

5. Recommendations

Further research can be carried out by considering the following;

1) Effect of heat and mass transfer on unsteady MHD Nanofluid flow via convergent-divergent channel under strong magnetic field.
2) Effect of heat and mass transfer on unsteady MHD Nanofluid of compressible flow through convergent-divergent channel.
3) Effect of skin friction coefficient, Nusselt and Prandtl number on unsteady MHD Nanofluid flow through convergent-divergent channel with heat and mass transfer.

References

[1] Alves. H. (1942). Existence of Electromagnetic.

[2] Hartmann. (1937). Hydrodynamic waves. Math.-fys. Medd. Vol 15, no. 6, pp. 405-406.

[3] Ella, R., (2013). The effects of MHD and Temperature Dependent Viscosity on the flow of non-Newtonian Nanofluid in a pipe. Analytical solution, Appl. Math. Model. 37, 3, pp 1451-1467.

[4] Makinde O. D. (2013). Buoyancy Effects on MHD Stagnation Point Flow and Heat Transfer of Nanofluid Past a convectively Heated Stretching /Shrinking Sheet. International Journal of Heat and Mass Transfer. Volume 62. Pp 33 (1), 526-533.

[5] Sheikholeslami, M., Ganji, D. D., Ashorynejad, H. R. Rokni, H. B. (2012). Analytical Investigation of Jeffrey-Hamel Flow with High Magnetic Field and Nanoparticle by Adomian Decomposition Method. App. Math. Mech 33 (1), pp 25-36.

[6] Hey, Shira Zaki M, Liu H, Himeno R, Sun Z (2006). A Numerical Coupling Model to Analyze the Blood Flow, Temperature and Oxygen Transport in Human Breast Tumor Under Laser Irradiation. Com Biol Medi 36: pp 130-135.

[7] Szasz A. (2007). Hyperthermia, a Modality in the Wings. J Cancer Res ther 3: pp 56-66.

[8] Y. Pathat, (2009). Recent Development in Nanoparticle Drug Delivery System, in Drug Delivery Nanoparticle Formulation and Characterization, pp. 1-7, Informa Health Care USA, New York.

[9] Mburu. A. Njeri, Thomas T. M. Onyango, Jackson Kwanza (2016). Investigation on Magneto hydrodynamic Flow Through Converging-Diverging Channel Under Weak Magnetic Field. LAP LAMBERT Academic Publishing, Saarbrucken. ISBN (N978-3-330-33677-3).

[10] Muhammad U, Syed T. M. D, Tamour Z. Muhammad. H. W. W (2018). Fluid Flow and Heat Transfer Investigation of Blood with Nanoparticle through Porous Vessels in the presence of Magnetic Field. Journal of Algorithms Computational Technology Volume 13: 1-15.

[11] Virginia M. Kitetu, Thomas T. M. Onyango, Jackson Kwanza (2020). Control Volume Analysis of MHD Nanofluid Flow as a Result of a stretching Surface and Suction.

[12] Edward Onyango, Mathew N. Kinyanjwi, Mark Kimathi, Surindar M. Uppal (2020). Unsteady Jeffrey-Hamel Flow in the Presence of Oblique Magnetic Field with Suction and Injection. Applied and Computational Mathematics; 9 (1): 1-13.

[13] Nidal H. Abu-Hamdel A. R. Bantan, Ferhand Aalizadeb, Ashkan Alimoradi (2020). Controlled Drug Delivery Using the Magnetic Nanoparticles in Non-Newtonian Blood Vessels, Alexandria Engineering Journal. Vol 59, pp 4049-4062.

[14] Ashish Mishra, Alok K. Pandey, Ali, Ali J. Chamkha Manoj Kumar (2020). Roles of Nanoparticle and Heat Generation/Absorption on MHD Flow of Silver-Water Nanofluid via Porous Stretching/Shrinking convergent/Divergent channel. Journal of the Egyptian Mathematical Society Volume 28. Article Number: 17.

[15] Misra JC, Sinha A, Shit GC. (2010). Flow of a Biomagnetic Viscoelastic Fluid. Application to Estimation of the Blood Flow in Arteries During Electromagnetic Hyperthermia, a Therapeutic Procedure for Cancer Treatment. Appl. Math Meth. Ed (31) pp 1401-1420.

[16] Jafari, A., Zamankhan, P., MO Usavi, S. M., Kolari. P (2009). Numerical Investigation of the Blood Flow. Part II: In Capillaries. Communication in non-Linear Science and Numerical simulation, 14 (4), 1396-1402.

[17] Wernet, V, Schaf, O., Ghobark, H, H, H., Denoyel, R (2005). Adsorption Properties of Zeolites for Artificial Kidney. Application Micro Porous Material 83 (1-3), 101-113.

[18] Brinkman, H. C. (1952). The Viscosity of Concentration Suspensions and Solutions. The Journal of Chemical Physics. 20 (4) 571-581.